Stabilisation analysis of multiple car-following model in traffic flow*

Peng Guang-Han(彭光含)†

College of Physics and Electronic Science, Hunan University of Arts and Science, Changde 415000, *China*

(Received 17 September 2009; revised manuscript received 23 October 2009)

An improved multiple car-following model is proposed by considering the arbitrary number of preceding cars, which includes both the headway and the velocity difference of multiple preceding cars. The stability condition of the extended model is obtained by using the linear stability theory. The modified Korteweg–de Vries equation is derived to describe the traffic behaviour near the critical point by applying the nonlinear analysis. Traffic flow can be also divided into three regions: stable, metastable and unstable regions. Numerical simulation is in accordance with the analytical result for the model. And numerical simulation shows that the stabilisation of traffic is increasing by considering the information of more leading cars and there is unavoidable effect on traffic flow from the multiple leading cars' information.

Keywords: traffic flow, optimal velocity model, numerical simulation

PACC: 6470, 0550, 0520

1. Introduction

Traffic flow is an interesting problem of modern society. To explain the complex properties of traffic, various traffic models have been developed, such as the cellular automaton models, car-following models, hydrodynamic models and gas kinetic models.[1,2] The car-following model is one of the favorable microscopic traffic models that depict the motion of cars by differential equations. The optimal velocity (OV) model proposed by Bando *et al.*,[3] as one of car-following models, has successfully described the formation of traffic jams and revealed the simplistic transition mechanism. The phase transitions between the freely moving traffic and jammed traffic have been clarified by linear stability analysis. Subsequently, much work has been done based on the OV model.[4−36] Among them, some induced by headways,[4−15] others considered velocity difference.[16−31] Also, the interactions of both headways and velocity differences were taken into account in a few models.[32−35]

In this study, drivers may obtain multiple information of headways and velocity differences from leading vehicles by making use of the intelligent transportation system (ITS). Based on considering the effect of multiple information of leading vehicles, we propose a multiple car-following (MCF) model. Linear stability analysis shows that this new model is more stable than previous ones. Numerical simulation also shows that our model is more reasonable than others.

The paper is organised as follows. We review the performance of the previous car-following models on the evolution of congestion in Section 2. In Section 3, the improved car-following model is presented. In Section 4, linear stability analysis is conducted. In Section 5, nonlinear analysis is done. Both analytic and numerical methods of this model are used to analyse some observed physical features which exist in real traffic in Section 6. Finally we conclude the paper in Section 7.

2. Previous car-following models

2.1. The optimal velocity model

In 1995, Bando *et al.* proposed a simple microscopic traffic model called the optimal velocity model (for short, OV model).[3] It was based on the idea that each vehicle has an optimal velocity, which depends on the following distance of the preceding vehicle. The motion of a vehicle n is described by the following equation:

$$\frac{\mathrm{d}v_n(t)}{\mathrm{d}t} = a\left[V(\Delta x_n) - v_n(t)\right], \tag{1}$$

*Project supported by the Natural Science Foundation of Hunan Province, China (Grant No. 07JJ6106), the Important Project of Scientific Research Foundation of Hunan University of Arts and Science, China (Grant No. JJZD0902) and the Fund of the 11th Five-year Plan for Key Construction Academic Subject of Hunan Province, China (Grant No. 06GXCD02).

†Corresponding author. E-mail: pengguanghan@yahoo.com.cn

© 2010 Chinese Physical Society and IOP Publishing Ltd

where $x_n(t)$ is the position of car n at time t, $\Delta x_n = x_{n+1} - x_n$ is the headway between car $n+1$ and car n at time t, a is the sensitivity of a driver, and V is the optimal velocity function (OVF). Bando *et al.* adopted an optimal velocity function as:[3]

$$V(\Delta x_n) = 0.5V_{\max}[\tanh(\Delta x_n - h_c) + \tanh(h_c)], \quad (2)$$

where $h_c = 2$ is the safety distance and $v_{\max}$ is the maximal velocity.

2.2. Xue's model

By taking relative velocity into account, Xue *et al.* developed an extended model.[18−20] The dynamic equation of a vehicle n is as follows:

$$\frac{\mathrm{d}v_n(t)}{\mathrm{d}t} = a\,[V(\Delta x_n) - v_n(t)] + \lambda \Delta v_n, \quad (3)$$

where λ is a sensitivity coefficient different from a. $\Delta v_n(t)$ is the velocity difference between the preceding vehicle $n+1$ and the following vehicle n, $\Delta v_n(t) = v_{n+1} - v_n$. Numerical simulation shows that the relative velocity in the Xue's model can stabilise traffic flow and decrease the number of jamming phases.[18−20] They derived the modified Korteweg-de Vries (mKdV) equation for describing the traffic jam in unstable region. In addition, Jiang *et al.*[17] presented a same simplified OV model for investigating the effects of the relative velocity, which is different from Xue's model at the sensitivity coefficient.

3. Model

Recently, by applying the ITS, drivers can receive information of other cars on the roads. Several traffic flow models have been proposed involving the use of ITS information[8−15,29−35] to enhance the stability of traffic flow. Therefore, we put forward a more useful model called the multiple car-following model (MCF model), which performs more realistically in the dynamical evolution of congestion by taking into account the multiple information of preceding leading vehicles through the ITS application. Evidence shows that this new model is theoretically an improvement over the Xue's model, and retains many strong points of the previous ones. The dynamics equation shows as follows:

$$\begin{aligned}&\frac{\mathrm{d}v_n(t)}{\mathrm{d}t}\\ &= a\,[V(\Delta x_n, \Delta x_{n+1}, \ldots, \Delta x_{n+m-1}) - v_n(t)]\\ &\quad + \lambda G(\Delta v_n, \Delta v_{n+1}, \ldots, \Delta v_{n+m-1}), m \ll n, \quad (4)\end{aligned}$$

where m is the number of the front vehicles total considered in our model. $V(\bullet)$ represents optimal velocities of considering m preceding vehicles. Equation (4) shows that the optimal velocities of the preceding vehicles are integrated into one synthesised optimal velocity function $V(\bullet)$, which is assumed in a linear form

$$\begin{aligned}&V(\Delta x_n, \Delta x_{n+1}, \ldots, \Delta x_{n+m-1})\\ &= p_1 V(\Delta x_n) + p_2 V(\Delta x_{n+1}) + \ldots p_m V(\Delta x_{n+m-1}).\end{aligned} \quad (5)$$

$G(\bullet)$ is a generic, monotonically increasing function, and assumed to have a linear form as:

$$\begin{aligned}&G(\Delta v_n, \Delta v_{n+1}, \ldots, \Delta v_{n+m-1})\\ &= q_1 \Delta v_n + q_2 \Delta v_{n+1} + \ldots q_m \Delta v_{n+m-1}, \quad (6)\end{aligned}$$

where

$$\begin{aligned}&\sum_{l=1}^{m} p_l = 1, \quad p_l = \begin{cases} \dfrac{p-1}{p^l}, & \text{for } l \neq m,\\ \dfrac{1}{p^{l-1}}, & \text{for } l = m,\end{cases}\\ &\sum_{l=1}^{m} q_l = 1, \quad q_l = \begin{cases} \dfrac{q-1}{q^l}, & \text{for } l \neq m,\\ \dfrac{1}{q^{l-1}}, & \text{for } l = m,\end{cases}\end{aligned} \quad (7)$$

p_l and q_l are the weighting values, $0 \leq p_l \leq 1$ and $0 \leq q_l \leq 1$, which mean the intensity of driver reacting to preceding vehicle l. In our paper, $p = 2, 3, 4, \ldots$ and $q = 2, 3, 4, \ldots$ being a constant. It is well known that the influence of the vehicle ahead on the vehicle motion reduces gradually as the distance between the considered vehicle and the vehicle ahead increases, which means $p_l > p_{l+1}$ and $q_l > q_{l+1}$. Also, the proper values of p_l and q_l could lead to desirable results. The model (4) conforms to the Xue's model if $m = 1$, which only considers the effect of the nearest-neighbor ahead car.

4. Linear stability analysis

Linear stability analysis can be conducted for the MCF model as follows. It is obvious that the vehicles move with the uniform headway b and the optimal velocity $V(b, b, \ldots, b)$ is the steady state solution for Eq. (4), which is given as:

$$x_n^0(t) = bn + V(b, b, \ldots, b)t \text{ with } \ b = L/N, \quad (8)$$

where N is the total number of vehicles, and L is the road length. Suppose $y_n(t)$ to be a small deviation from the steady-state solution $x_n^0(t)$: $x_n(t) = x_n^0(t) + y_n(t)$. Substituting it and Eqs. (5), (6) and (8) into Eq. (4) and linearising the resultant equation yields.

$$y_n''(t) = a\left[\sum_{l=1}^{m} p_l V'(b)\Delta y_{n+l-1} - y_n'(t)\right] + \lambda\left(\sum_{l=1}^{m} q_l \Delta y_{n+l-1}'\right), \quad (9)$$

where $\Delta y_n = y_{n+1}(t) - y_n(t)$, and $V'(b) = \mathrm{d}V(\Delta x_n)/\mathrm{d}\Delta x_n\,|_{\Delta x_n = b}$. By expanding $y_n(t)$, $y_n(t) = \mathrm{e}^{(\mathrm{i}\alpha_k n + zt)}$, in the Fourier-models:

$$z^2 + \left(a - \lambda\left(\sum_{l=1}^{m} q_l(\mathrm{e}^{\mathrm{i}kl} - \mathrm{e}^{\mathrm{i}k(l-1)})\right)\right) z - aV'(b)\left(\sum_{l=1}^{m} p_l(\mathrm{e}^{\mathrm{i}kl} - \mathrm{e}^{\mathrm{i}k(l-1)})\right) = 0, \quad (10)$$

where $z = z_1(\mathrm{i}k) + z_2(\mathrm{i}k)^2 + \ldots$, and inserting them into Eq. (4) we have the first- and second-order terms of coefficients in the expression of z respectively as follows:

$$z_1 = V'(b),$$
$$z_2 = \frac{a\sum_{l=1}^{m} p_l(2l-1) + 2\lambda\sum_{l=1}^{m} q_l}{2a} V'(b) - \frac{(V'(b))^2}{a}. \quad (11)$$

If z_2 is a negative value, the uniform steady-state flow becomes unstable for long-wavelength modes, while the uniform flow is stable when z_2 is a positive value. Thus the neutral stability condition is:

$$V'(b) = \frac{a}{2}\sum_{l=1}^{m} p_l(2l-1) + \lambda. \quad (12)$$

For small disturbances with long wavelengths, the uniform traffic flow is stable if

$$V'(b) < \frac{a}{2}\sum_{l=1}^{m} p_l(2l-1) + \lambda. \quad (13)$$

When $m = 1$, the result of stable conditions is the same as that of Xue's model:[18]

$$V'(b) < \frac{a}{2} + \lambda. \quad (14)$$

Comparing the result with that of Xue's model, we can conclude that the improved model is stabilised in the region $a/2 + \lambda < V'(b) < a/2\sum_{l=1}^{m} p_l(2l-1) + \lambda$ by the effect of introducing the multiple information of preceding vehicles, which means that the traffic flow becomes more stable than that in Xue's model by introducing the multiple information of preceding vehicles into original car-following model. It can also be obtained that the more the number of preceding leading cars are considered, the more stable the traffic will be.

The neutral stability line (solid line) in the parameter space (b, a) for different m, as $m = 1, 2, 3, 5$ respectively, is shown in Fig. 1. Where $\lambda = 0.1$ and $p = 5$. The neutral stability criterion presents the jamming transition curve among the free traffic, the inhomogeneous coexisting phase, and the homogeneous congested traffic. The apex of each curve indicates the critical point. The traffic flow is stable above the neutral stability line and a traffic jam will not appear. While below the line, traffic flow is unstable and the density waves emerge. In addition, once the homogeneous traffic flow becomes unstable, the traffic flow evolves in time into an inhomogeneous jamming phase, which is characterised by the presence of an alternation pattern (congestion cluster) of high-density and low-density regions, and all vehicles in the platoon enter into a state of stop-and-go traffic after enough time. From Fig. 1, it can be seen that the more vehicles ahead are taken into account, the more the critical points and the neutral stability curves are lowered, which means that the more we consider the effects of information of preceding leading cars, the more stable the traffic will be. The traffic jam is thus suppressed efficiently. When m=1, the neutral stability line is the same as that of the Xue's model in single-lane freeway.

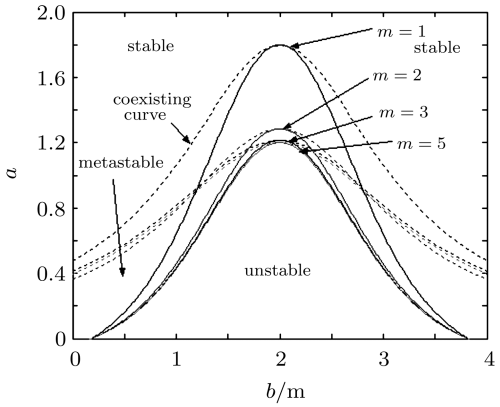


Fig. 1. The schematic profile of the phase diagram in the parameter space (Δx, a).

Theoretically speaking, with the increasing value of m, the traffic flow is more stable. However, with

the increasing value of m, the information of more preceding leading vehicles need be collected and processed too. According to Fig. 1, when $m = 3, 5$, corresponding curves are almost coincided, which shows that the information of only three preceding leading vehicles ($m = 3$) is enough to make the traffic sufficiently stable under small disturbance, which is same as the result of cooperative driving model that did not consider the velocity difference in Ref. [8]. However, many references[16−35] have verified that velocity difference has played important role in car-following models, which also shows that MCF model is obviously superior to cooperative driving model. Therefore, $m = 3$ is the optimal state in MCF model. That is to say, considering the effect of the three preceding leading vehicles on the following vehicle can suppress the traffic jam effectively as well as save the resource. Also it implies that this model is more useful with the consideration of effect of three preceding leading vehicles on the following car.

5. Nonlinear analysis

For convenience of later nonlinear analysis, we rewrite Eq. (4) as the following form:

$$\frac{\mathrm{d}^2(\Delta x(t))}{\mathrm{d}t^2} = a\left\{\sum_{l=1}^{m} p_l V(\Delta x_{n+l}) - \sum_{l=1}^{m} p_l V(\Delta x_{n+l-1})] - \frac{\mathrm{d}(\Delta x_n)}{\mathrm{d}t}\right\} + \lambda\left\{\sum_{l=1}^{m} q_l\left(\frac{\mathrm{d}(\Delta x_{n+l})}{\mathrm{d}t} - \frac{\mathrm{d}(\Delta x_{n+l-1})}{\mathrm{d}t}\right)\right. . \tag{15}$$

We apply the reductive perturbation method to Eq. (15) and focus on the system behaviour near the critical point (h_c, a_c). With such treatment, the nature of kink–antikink soliton solutions can be described by the mKdV equation. We introduce slow scales for space variable n and time variable t,[8,13] and define the slow variables X and T as:[8,13]

$$X = \varepsilon(n + bt), \tag{16}$$

$$T = \varepsilon^3 t, \tag{17}$$

where $\varepsilon = \sqrt{(a_c/a - 1)}$, $0 < \varepsilon \leq 1$, b is a constant to be determined. From the parabolic form of the neutral stability line near the critical point, it is expected that the amplitude of the density wave scales $c \propto \varepsilon$.[8,13] The headway is set as

$$\Delta x_n(t) = h_c + \varepsilon R(X, T). \tag{18}$$

Substituting Eqs. (16)–(18) into Eq. (15), and making the Taylor expansions to the fifth order of ε, we obtain the following nonlinear partial differential equation:

$$\varepsilon^2[b - V']\partial_X R + \varepsilon^3\left[\frac{b^2}{a} - \frac{V'}{2}\sum_{l=1}^{m} p_l(2l-1) - \lambda\frac{b}{a}\right]\partial_X^2 R + \varepsilon^4\left[\partial_T^2 R + \left[-\frac{V'}{6}\sum_{l=1}^{m} p_l(3l^2 - 3l + 1) - \lambda\sum_{l=1}^{m} q_l(2l-1)\frac{b}{2a}\right]\partial_X^3 R - \frac{V'''}{6}\partial_X R^3\right\} + \varepsilon^5\left\{\left(\frac{2b}{a} - \frac{\lambda}{a}\right)\partial_T\partial_x R + \left[-\frac{V'}{24}\sum_{l=1}^{m} p_l(4l^3 - 6l^2 + 4l - 1) - \frac{1}{24}\sum_{l=1}^{m} q_l(3l^2 - 3l + 1)\frac{\lambda b}{a}\right]\partial_X^4 R - \frac{V'''}{12}\sum_{l=1}^{m} p_l(2l-1)\partial_X^2 R^3\right\} = 0, \tag{19}$$

where $V' = \mathrm{d}V(\Delta x)/\mathrm{d}\Delta x|_{\Delta x = h_c}$, $V''' = \mathrm{d}^3 V(\Delta x)/\mathrm{d}\Delta x^3\big|_{\Delta x = h_c}$.

Near the critical point (a_c, h_c), with $b = V'$, $a_c/a = 1 + \varepsilon^2$ and eliminating the second- and third-order terms of ε from Eq. (19), equation (19) can be simplified as:

$$\varepsilon^4[\partial_T R - g_1 V'\partial_X^3 R + g_2\partial_X R^3] + \varepsilon^5[g_3\partial_X^2 R + g_4\partial_X^4 R + g_5\partial_X^2 R^3] = 0, \tag{20}$$

where

$$g_1 = \frac{1}{6}V' \sum_{l=1}^{m} p_l(3l^2 - 3l + 1) + \frac{1}{2}\sum_{l=1}^{m} q_l(2l-1)\lambda V'/a_c, \tag{21a}$$

$$g_2 = -\frac{V'''}{6}, \quad g_3 = \frac{1}{2}V' \sum_{l=1}^{m} p_l(2l-1), \tag{21b}$$

$$g_4 = \left(\frac{2V'}{a_c} - \frac{\lambda}{a_c}\right)\left[\frac{V'}{6}\sum_{l=1}^{m} p_l(3l^2-3l+1) + \frac{1}{2}\sum_{l=1}^{m} q_l(2l-1)\lambda V'/a_c\right] + \left[-\frac{1}{24}V'\sum_{l=1}^{m} p_l(4l^3-6l^2+4l-1) - \frac{1}{6}\sum_{l=1}^{m} q_l(3l^2-3l+1)\lambda V'/a_c\right], \tag{21c}$$

$$g_5 = -\frac{1}{12}V'''\left[\sum_{l=1}^{m} p_l(2l-1) - 4V'/a_c - 2\lambda\right]. \tag{21d}$$

In order to get the standard mKdV equation, we use the transformations

$$T' = g_1 T, \quad R = \sqrt{\frac{g_1}{g_2}}R'. \tag{22}$$

Substituting Eq. (22) into Eq. (20), we obtain the regularised equation:[8]

$$\partial_T R' - \partial_X^3 R' + \partial_X R'^3 + \varepsilon M[R'] = 0, \tag{23}$$

where

$$M[R'] = \sqrt{\frac{1}{g_1}}\left[g_3\partial_X^2 R' + \frac{g_1 g_5}{g_2}\partial_X^2 R'^3 + g_4\partial_X^4 R'\right]. \tag{24}$$

Equation (23) is the modified KdV equation with an $O(\varepsilon)$ correction term. Firstly, we ignore the $O(\varepsilon)$ term in Eq. (23) and get the mKdV equation with the kink-antikink soliton solution:

$$R'_0(X,T') = \sqrt{c}\tanh\sqrt{c/2}(X - cT'), \tag{25}$$

where c is the propagation velocity. In order to determine c for the solution of Eq. (23), the following requirement must be satisfied:[8,13]

$$\begin{aligned}&(R'_0, M[R'_0])\\ &= \int_{-\infty}^{+\infty} \mathrm{d}X R'_0(X,T')M[R'_0(X,T')]\\ &= 0,\end{aligned} \tag{26}$$

where $M[R'_0] = M[R']$. By solving the above equation, we obtain the selected velocity c for the kink–antikink solution according to the general solution presented by Ge *et al.*:[8]

$$c = 5g_2 g_3/(2g_2 g_4 - 3g_1 g_5). \tag{27}$$

Hence, the kink–antikink soliton solution is of the form ($V' = 1$, $V''' = -2$).[8,13]

$$\begin{aligned}&R(X,T)\\ &= \sqrt{\frac{g_1 c}{g_2}\left(\frac{a_c}{a} - 1\right)} \times \tanh\sqrt{c/2}(X - cg_1 T).\end{aligned} \tag{28}$$

Thus the general kink–antikink soliton of the headway, i.e., the mKdV equation, is obtained:

$$\begin{aligned}\Delta x_n(t) \;=\; & h_c + \sqrt{\frac{g_1 c}{g_2}\left(\frac{a_c}{a} - 1\right)} \times \tanh\sqrt{\frac{c}{2}\left(\frac{a_c}{a} - 1\right)}\\ & \times \left[j + V't - cg_1\left(\frac{a_c}{a} - 1\right)t\right].\end{aligned} \tag{29}$$

Here the amplitude A of the solution is:

$$A = \sqrt{\frac{g_1 c}{g_2}\left(\frac{a_c}{a} - 1\right)}. \tag{30}$$

The kink–antikink solution represents the coexisting phase, which consists of the freely moving phase at low density and the jammed (or congested) phase at high density. The headway of the freely moving phase and the jammed phase are given by $\Delta x = h_c + A$ and $\Delta x = h_c$–A, respectively. Thus, we can obtain the coexisting curve in the (Δx, a) plane (see Fig. 1). Komatsu and Sasa[37] and Muramats and Nagatani[38] showed that the traffic flow could be divided into three regions: stable, metastable and unstable regions. Our model also exhibits the similar regions as shown in Fig. 1. Therefore, the solution of the mKdV equation gives the coexisting curve in the jamming transition. When $m = 1$, the result is similar to that solved by Xue *et al.*[18]

6. Numerical simulation

A numerical simulation is carried out to observe the traffic dynamics in the MCF model. For comparison, we take the same parameters as those in Xue's model. There are $N = 100$ vehicles running on a road with the length $L = 200$, under a periodic boundary condition. We set the same initial disturbance as that in Ref. [18]:

$$x_N(0) = x_N^{(0)}(0) + 0.1,$$
$$x_n(0) = x_n^{(0)}(0), \quad (n \neq N), \tag{31}$$
$$\dot{x}_n(0) = 0. \tag{32}$$

Other parameters: $a = 1$, $\lambda = 0.1$, $b = L/N$, $p = 5$, $q = 4$.

Firstly, we consider the case of MCF model at different values of m. In order to get insight information of the variation of vehicles, the snapshots of the velocities of all vehicles at $t = 100$ s, $t = 300$ s and $t = 1000$ s for MCF model are shown in Figs. 2, 3 and 4, respectively. We clearly see from the figures that vehicle velocities tend to locate on the two typical values as time develops. The homogeneous flow eventually develops into congestion, which corresponds to stop-and-go traffic. However, we clearly observe the appearance of the amplitude of the curves decreasing, which shows that the more stable the uniform traffic flow is, with the increasing value of m from 1–3.

Secondly, the velocity-headway trajectory in the MCF model is compared to that in the Xue's model as follows. A closed trajectory called a hysteresis loop is clearly observed in Xue's model and MCF model, respectively. When the traffic flow becomes stationary after sufficiently large time, the motion of all vehicles forms a loop as shown in Figs. 5–7 separately. Changing the value of m, loops of different size can be obtained in MCF model [see Fig. 5], which shows that the more vehicles are taken into account, the smaller the area of loops is. The result is the same as the results in Ref. [18] when $m = 1$. From Fig. 6, it shows that the hysteresis loops become smaller with the decreasing of p and q at $m = 3$. When $p = 3$ and $q = 2$, criterion (13) is held, the traffic flow is stable, the hysteresis loop will not be generated, and in phase space, there will be only a point H on the optimal velocity curve instead. The unrealistic phenomena of the negative velocity appear if the condition of $a < 0.68$ is satisfied in Xue's model according to Fig. 7. From Fig. 7, the unrealistic negative velocity can disappears in MCF model by considering the multiple information of leading vehicles. From this point of view, MCF model describes the traffic dynamics more exactly when the value of m over 1, which furthermore verifies that the modification of Xue's model is more reasonable and realistic than previous ones. Obviously, a decreases with the increasing value of m under stable traffic flow.

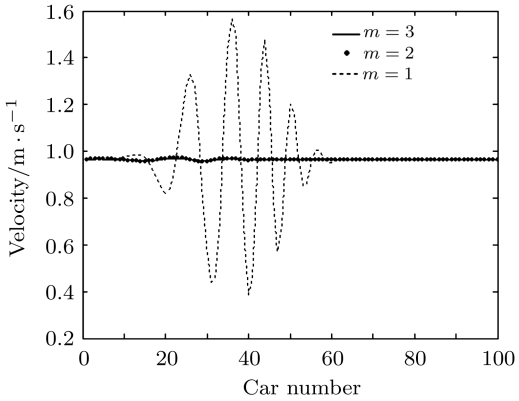


Fig. 2. Snapshot of the velocities of all vehicles at different values of m when $t = 100$ s in MCF model.

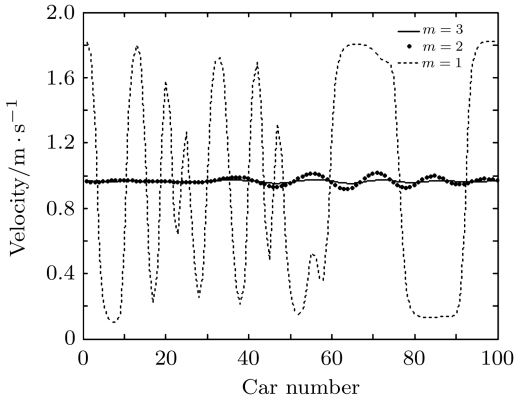


Fig. 3. Snapshot of the velocities of all vehicles at different values of m when $t = 300$ s in MCF model.

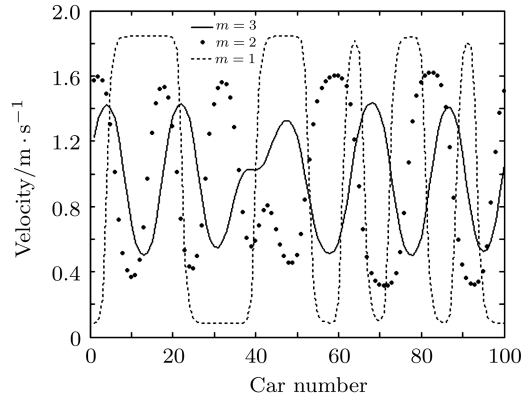


Fig. 4. Snapshot of the velocities of all vehicles at different values of m when $t = 1000$ s in MCF model.

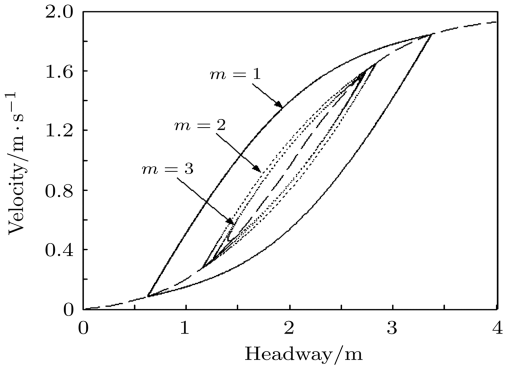


Fig. 5. Loops for the MCF model at different values of m. The dashed curve represents OVF.

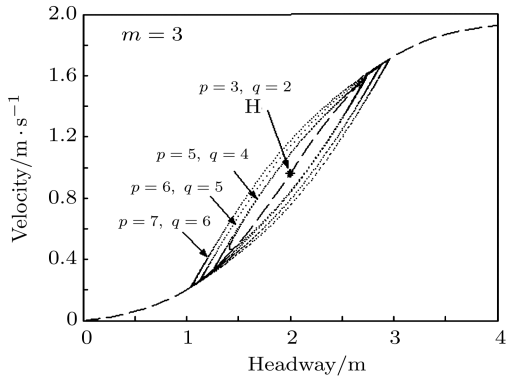


Fig. 6. Loops for the MCF model at different values of p and q when $m = 3$. The dashed curve represents OVF.

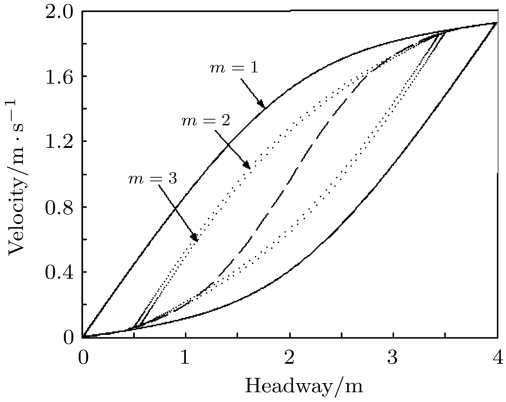


Fig. 7. Loops for the MCF model at different values of m when $a = 0.68$. The dashed curve represents OVF.

Finally, the plot of the headway versus car number is given at two different large times in Fig. 8 when $p = 4$ and $q = 3$. In patterns (a) and (b), the traffic flow is unstable because the stability condition is not satisfied for $m = 1, 2$. When a small disturbance is introduced into the homogeneous traffic flow, the traffic flow evolves into the inhomogeneous traffic flow due to the amplification of the perturbation after sufficiently long time. In patterns (c) and (d), the traffic flow is stable for $m = 3,\ 4$. So our conclusion is that the

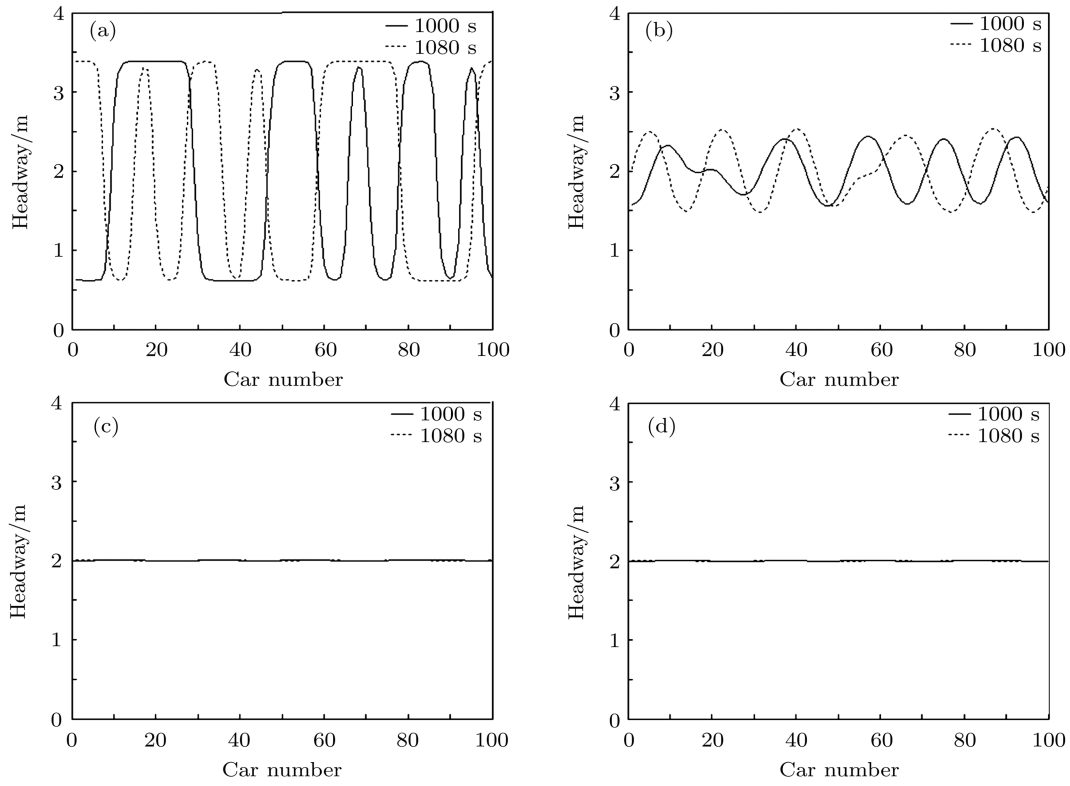


Fig. 8. The headway profiles of all cars at $t = 1000$ s and $t = 1080$ s for $m = 1, 2, 3, 4$.

uniform traffic flow is getting more and more stable with the number of the considered front vehicles increasing in the pattern (a) to (d). It is not enough for suppressing the traffic congestion that only the next-nearest-neighbor interaction is taken into account with the same sensitivity in this simulation.

From Fig. 8, we can also see that the kink–antikink soliton solution appears as traffic jams. In the headway profiles, the two curves at $t = 1000$ s and $t = 1080$ s exhibit the same shape and the propagation direction is backwards, which is obviously seen from patterns (a) and (b). The amplitude of the density waves decreases with the number of the considered front vehicles increasing in the pattern (a) to (d). Moreover the two curves in patterns (c) and (d) are coincided and the density waves disappear. The traffic jams are suppressed effectively by considering more interactions.

7. Conclusions

We introduce an improved MCF model for a single lane car-following theory which is more realistic than the Xue's model by taking the multiple information of leading vehicles into account. Linear stability analysis has been done and the stable criterion is given. The kink–antikink soliton solution of the mKdV equation near the critical point is derived to describe the traffic jams. The kink–antikink soliton solution appeared as traffic jams and the propagation direction of the density waves are exhibited in the same pattern. From the numerical simulation, we can conclude that the stabilisation of traffic is increasing efficiently by taking into account the information of more leading cars. Also simulation results directly indicate that the preceding vehicles term has an important impact on the traffic dynamics.

References

[1] Chowdhury D, Santen L and Schadschneider A 2000 *Phys. Rep.* **329** 199
[2] Helbing D 2001 *Rev. Mod. Phys.* **73** 1067
[3] Bando M, Hasebe K, Nakyaama A, Shibata A and Sugiyama Y 1995 *Phys. Rev.* E **51** 1035
[4] Li X L, Song T, Kuang H and Dai S Q 2008 *Chin. Phys.* B **17** 3014
[5] Hayakawa H and Nakanishi K 1998 *Prog. Theor. Phys. Suppl.* **130** 57
[6] Nagatani T 1999 *Phys. Rev.* E **60** 6395
[7] Lenz H and Wagner C K 1999 *Eur. Phys. J.* B **7** 331
[8] Ge H X, Dai S Q, Dong L Y and Xue Y 2004 *Phys. Rev.* E **70** 066134
[9] Wagner C K 1998 *Physica* A **260** 218
[10] Nakayama A, Sugiyama Y and Hasebe K 2001 *Phys. Rev.* E **65** 016112
[11] Hasebe K, Nakayama A and Sugiyama Y 2003 *Phys. Rev.* E **68** 026102
[12] Sawada S 2002 *Int. J. Mod. Phys.* C **13** 1
[13] Ge H X, Dai S Q, Xue Y and Dong L Y 2005 *Phys. Rev.* E **71** 066119
[14] Zhu H B and Dai S Q 2008 *Physica* A **387** 3290
[15] Ge H X, Zhu H B and Dai S Q 2006 *Eur. Phys. J.* B **54** 503
[16] Helbing D and Tilch B 1998 *Phys. Rev.* E **58** 133
[17] Jiang R, Wu Q S and Zhu Z J 2001 *Phys. Rev.* E **64** 017101
[18] Xue Y 2003 *Acta. Phys. Sin.* **52** 2750 (in Chinese)
[19] Xue Y, Dong L Y, Yuan Y W and Dai S Q 2002 *Acta. Phys. Sin.* **51** 492 (in Chinese)
[20] Xue Y 2002 *Chin. Phys.* **11** 1128
[21] Tang T Q, Huang H J and Gao Z Y 2005 *Phys. Rev.* E **72** 066124
[22] Wang T, Gao Z Y and Zhao X M 2006 *Acta. Phys. Sin.* **55** 634 (in Chinese)
[23] Li L and Shi P F 2005 *Chin. Phys.* **14** 0576
[24] Zhao X M and Gao Z Y 2005 *Eur. Phys. J.* B **47** 145
[25] Li Z P and Liu Y C 2006 *Chin. Phys.* **15** 1570
[26] Sawada S 2006 *Int. J. Mod. Phys.* C **17** 65
[27] Li Z P, Liu Y C and Liu F Q 2007 *Int. J. Mod. Phys.* C **18** 819
[28] Li Z P, Gong X B and Liu Y C 2006 *Commun. Theor. Phys.* **46** 367
[29] Lei Y and Shi Z K 2008 *Chaos, Solitons and Fractals* **36** 550
[30] Gong H X, Liu H C and Wang B H 2008 *Physica* A **387** 2595
[31] Ge H X 2008 *Physica* A **360** 1
[32] Zhu W X and Liu Y C 2008 *J. Shanghai Jiaotong Univ. (Sci.)* **13** 166
[33] Xie D F, Gao Z Y and Zhao X M 2008 *Commun. Comput. Phys.* **3** 899
[34] Peng G H, Sun D H and He H P 2008 *Acta. Phys. Sin.* **57** 7541 (in Chinese)
[35] Mo Y L, He H D, Xue Y, Shi W and Lu W Z 2008 *Chin. Phys.* B **17** 4446
[36] Tang T Q, Huang H J, Wong S C and Jiang R 2009 *Chin. Phys.* B **18** 975
[37] Komatasu T and Sasa S 1995 *Phys. Rev.* E **52** 5574
[38] Muramatsu M and Nagatani T 1999 *Phys. Rev.* E **60** 180